Engineering Structures 179 (2019) 296–309

Contents lists available at ScienceDirect

Engineering Structures

journal homepage: www.elsevier.com/locate/engstruct

Seismic duration effect on damping reduction factor using random vibration theory

Rita Greco[a], Ivo Vanzi[b], Davide Lavorato[c], Bruno Briseghella[d,*]

[a] DICATECH, Department of Civil Engineering, Environmental, Territory, Building and Chemical, Technical University of Bari, Via Edoardo Orabona, 4, 70126 Bari, Italy
[b] InGeo Engineering and Geology Department, University of Chieti-Pescara "G. d'Annunzio", Viale Pindaro 42, 65127 Pescara, Italy
[c] Dept. of Architecture, Roma Tre University, Largo GB Marzi 10, 00153 Rome, Italy
[d] College of Civil Engineering, Fuzhou University, No. 2 Xue Yuan Road, 350108 Fuzhou, Fujian Province, PR China

ARTICLE INFO

Keywords:
Ground motion duration
Damping reduction factor
Seismic response spectrum
Stochastic process
Random vibration theory

ABSTRACT

Damping Reduction Factor plays a key role in scientific literature and Technical Codes, but till now existing formulations present differences and inconsistences probably because obtained by integration of real recorded events, thus sensible to specific used data. This paper investigates the relation between damping reduction factor and earthquake duration by means of random vibration theory. A stochastic process, that is non-stationary and filtered, is used to model a seismic event. The modulation function is suitably chosen to describe earthquakes characterized by different durations. The stochastic process peak theory allows to calculate damping reduction factor after the definition of the probabilistic response of a simple linear visco-elastic oscillator. The variability with seismic duration for different soil conditions and damping ratios is investigated. The study points out that damping reduction factor is more sensitive to seismic duration in the range of high period and on rigid soil with respect to other conditions. The results show that, if damping ratio or effective duration values are increased, the damping reduction factor value diminishes.

1. Introduction

Serious seismic damage observed on structures and infrastructures systems up to today [1] can be prevented by means of retrofitting interventions if the capacity of these systems and the seismic demand are properly evaluated [2–6] In structural seismic design, Damping Reduction Factor (DRF) represents an effective tool for design purposes to estimate the demand by response spectra characterized also by damping ratios different from 5% as in the case of structures equipped with passive energy dissipation or isolation systems. DRF modifies the values of the conventional elastic spectral response with damping ratio equal to 5% to the values corresponding to a different 7 damping level. It is defined as the ratio between the spectral ordinate at 5% conventional damping and the spectral ordinate at a different level of damping.

DRF finds many applications to study the behavior of structures [7], especially for the ones equipped with passive energy dissipation or isolation systems [8–12]. In these situations, the DRF permits to estimate the variation of the structural response (displacements and forces) due to the high supplemental damping values [5,13–15] In addition, for inelastic structures, DRF allows to calculate the maximum displacement demand from the one of an equivalent linear system [8]. For these and other reasons the DRF is particularly suitable for the seismic design of a structure since it provides a practical evaluation of the reduction of earthquake loads for effects of structural, non-structural and supplementary energy dissipation systems. For that reason, it is selected as a key parameter in the present study.

In past years, several studies for the formulation of the DRF have been carried out by many researchers, the outcomes of which have been adopted by the main seismic codes. Different expressions for the DRF can be found in literature. Up to today, the main research efforts have been oriented to the study of the response of a simple (elastic) SDOF system with viscous damping under seismic action [16–22]. As a consequence, the codes introduce a DRF that depends on the damping ratio only, whereas different authors [20–22] showed that various parameters may affect the DRF. There are two ways to classify the parameters that \ influence the DRF: by non-structural parameters such as earthquake magnitude, ground motion duration (GMD), site conditions, epicentral distance, etc. or by structural parameters such as damping of the structure, natural vibration period, dissipation device properties (energy dissipation capacity), etc. A very interesting topic is represented by the dependence of DRF on seismological parameters. This dependence is particularly evident considering local site conditions,

* Corresponding author.
E-mail addresses: rita.greco@poliba.it (R. Greco), i.vanzi@unich.it (I. Vanzi), davide.lavorato@uniroma3.it (D. Lavorato), bruno@fzu.edu.cn (B. Briseghella).

https://doi.org/10.1016/j.engstruct.2018.10.074
Received 1 May 2018; Received in revised form 26 October 2018; Accepted 28 October 2018

source distance and magnitude of the earthquake [20–23]. In [24] a simulation procedure to estimate the DRF based on an artificial neural network has been developed. The effect of magnitude on DRF is greater in the case of large earthquakes as it was pointed out in different studies [21] for structures with natural periods greater than 0.5 sec. Attention should be placed to the case of structures with shorter natural periods (< 0.5 sec) for which the magnitude can have also contrary effects [22]. Concerning the influence of seismological parameters on DRF, Bommer et al. [21] focused their studies on the GMD. The authors observed that it is possible to take into account the influence of magnitude and distance by studying the effect of the GMD and the number of cycles. Based on this observation, Stafford et al. [25] introduced significant equations that give the DRF for different damping ratios starting from the number of cycles and the GMD. In its research, Stafford concluded that a prediction model based on the GMD parameter could be used with difficulties as this parameter usually is not one of the parameters elaborated and directly available in earthquake databases. However, non - distinction between soil types is given by Stafford et al. [25]. Rosenblueth [26] suggested an equation to predict the influence of GMD on DRF and, in accordance with Stafford et al. [25], concluded that the influence of GMD appears negligible for earthquake GMD larger than about 20 sec.

The GMD finds a different definition in the models proposed by Stafford et al. [25] and Rosenblueth [26] but a very good match is observed for damping ratio equal to 10%. Some discrepancies are noticeable among the two models when damping ratio increases. The influence of GMD on DRF has been also investigated by Anbazhagan et al. [27]. The authors choose the pseudo-spectral acceleration to define the DRF and investigate how the DRF varies as a function of magnitude and GMD, distance of earthquake hypocenter, classification of site (soil type), period and damping. The dependence of DRF on the GMD was also analyzed by Daneshvar et al. [28] which concluded that DRF mainly depends on the GMD and the frequency content that are different for each record. Zhou et al. [29] studied how the DRF is affected by the effective GMD. The authors pointed out that greater values of the damping ratio or of the effective GMD produce smaller values of DRF. However, the GMD is in turn function of ground motion distance and magnitude and of soil type, that are parameters much more common and available in earthquake databases. For that reason, it is usually preferred to introduce a function including these parameters in order to define the DRF, indirectly indicating also a relation between DRF and GMD. Conversely, in this study the authors investigate the direct dependence of DRF on GMD, but also including the influence of soil type.

Rezaeian et al. [30] propose a model to relate the DRF to magnitude and distance to include in the model the high influence of GMD. The influence of different parameters on DRF is not the same in the cited studies because the sites are classified in different way and the selection of ground motions is performed by different criteria. So a stochastic process is adopted in the proposed study to overcome this difficulties.

In a previous study [31] the authors, by means of the random theory approach, investigated the effect of soil type on DRF and demonstrated that not only the predominant frequency of the seismic event but also the bandwidth of seismic signal affect the DRF. Since the study of the joint effect on DRF of parameters such as soil type and GMD has not performed in other studies, the authors will apply the random vibration theory to analyse in a combined way the influence of earthquake duration and soil type on DRF. GMD is a key parameter in seismic design. Since the 1950s, the peak acceleration, frequency content and GMD are considered important parameters to design the structures but, up to today, peak acceleration and frequency content are the only parameters used in design methods. The influence of GMD on DRF is investigated in the present study by means of the random vibration theory: a modulated filtered stochastic process is applied on a linear single degree of freedom (SDF) system and the peak theory of stochastic process is used to calculate the seismic spectrum in stochastic terms. The product of a time modulation function [32,33] and a stationary filtered stochastic process gives a modulated non-stationary stochastic process. A series of two linear oscillators forced by a modulated white noise process allows to obtain the linear fourth order filter that is adopted in the procedure. A formulation correlating the modulating function and the GMD through the Arias intensity [41] is introduced to analyze the effects of the GMD on DRF. In this way, the stochastic dynamic response can be evaluated for different GMDs, properly defining the modulation function and therefore a sensitivity analysis on DRF can be carried out to evaluate how DRF changes as a function of different parameters. The proposed approach overcomes the limitations of the strategies based on seismic records of real events; in fact in these it is difficult to accurately identify the influence of different factors. This is pointed out by the discrepancies among the various studies existing in the scientific literature.

The main advantage of using a stochastic approach is, on the contrary, the possibility to represent seismic motion by a simple model defined by few parameters, but able to describe the most seismological characteristics of real earthquakes as content of energy, frequency and GMD. On the other hand, the proposed approach would require an assessment of the spectrum parameters themselves on the basis of seismic models that are more consistent with the seismic scenario.

The study is presented in the following sections: the stochastic model of the seismic acceleration is explained in Section 2. The relation between the modulation function parameters and GMD is defined in Section 3. The evaluation of DRF in stochastic terms is developed in Section 4. The results of the sensitivity analysis developed considering different GMDs and soil conditions are shown and then discussed in Section 5. A formulation for DRF evaluation useful for practical applications is proposed and compared with other existing formulations in Section 6. Finally, conclusions are given in Section 7.

2. Stochastic modelling of seismic motion

It is well known that earthquake ground motion is a classic example of a non-stationary stochastic process with temporal variation of both amplitude and frequency characteristics. The most common way to model an earthquake accelerogram consists in expressing it by a simple product of a stationary signal and a deterministic envelope function, i.e. the modulation function, so obtaining a uniformly modulated stochastic process. The stationary signal is generally modeled by a Gaussian stationary white noise process $W(t)$ which passes through a linear filter in order to obtain the desired power spectral density function. The parameters of the filter are chosen so as to shift the energy of the accelerogram in the frequency ranges that are excited at the site. The modulation function $\phi(t)$ allows to obtain the desired time-dependent amplitude of the stationary filtered process and aims at reproducing the shape of the energy build-up, strong-motion duration and decay of earthquakes at the site.

Seismic acceleration is assumed as a uniformly modulated non-stationary stochastic process that is calculated by the product of a time modulation function $\phi(t)$ and a stationary process [34]. The stationary part of the process is described by the well known filtered process proposed by Clough et al. [35]: two linear oscillators in series, subjected to a modulated white noise process give a linear fourth order filter. Ground acceleration $\ddot{X}_g$ is given by:

$$\begin{cases} \ddot{X}_g(t) = -\omega_p^2 X_p(t) - 2\xi_p\omega_p \dot{X}_p(t) + \omega_f^2 X_f + 2\xi_f\omega_f \dot{X}_f(t) \\ \ddot{X}_p(t) + \omega_p^2 X_p(t) + 2\xi_p\omega_p \dot{X}_p(t) = \omega_f^2 X_f + 2\xi_f\omega_f \dot{X}_f(t) \\ \ddot{X}_f(t) + 2\xi_f\omega_f \dot{X}_f(t) + \omega_f^2 X_f = -\phi(t) W(t) \end{cases} \quad (1)$$

where $W(t)$ is the white noise stochastic process, with Power Spectral Density function S_0; $X_f(t)$ is the first filter response, with frequency ω_f and damping ratio ξ_f, $X_p(t)$ is the second filter response with frequency ω_p and damping ratio ξ_p; $\phi(t)$ is the modulation function. The present

research assumes the Jennings' modulation function [36], below reported:

$$\phi(t) = \alpha t e^{-\beta t}\ \alpha,\ \beta > 0 \tag{2}$$

α, β being the parameters that describe the shape of the modulation function that will be selected in Section 3.

It is useful to clarify that the modulation function used in this study is only one of a variety of forms that could be used to represent the time variation of earthquake signal. The modulation function commonly used are described in [36]. Moreover, even if the procedure was developed with reference to the Jennings' modulation function, a similar procedure, with the appropriate variations, could be extended also for other modulation functions present in literature, appropriately selecting the modulation function parameter.

3. Definition of modulation function considering the earthquake duration

Until now, GMD has been defined in different ways in literature [37] but the bracketed duration, the uniform duration and the significant duration are the most used. For a given curve that shows the values of the acceleration as a function of time, the duration of the ground motion is a time interval. In the case of bracketed duration, a threshold value of acceleration (usually 0.05 g) is defined.

The bracketed duration [38] is the time interval between the time corresponding to the first and the time corresponding to the last overrun of the defined threshold value of acceleration. The choice of the threshold value is different in literature and therefore this definition of GMD results subjective (it can be absolute or relative e.g. 10% of Peak Ground Acceleration (PGA)). The uniform duration [39,40] is calculated as the sum of time intervals. During each time interval the acceleration values overrun the threshold value of the acceleration. This definition of GMD is explained in a way similar to the bracketed duration except for the interval between the thresholds. The disadvantages in the use of this GMD definition are: the dependence of GDM on the chosen threshold acceleration value; the influence of small earthquakes recorded before or after the main earthquake record that could be included in the GMD evaluation. The effective duration is a preferable definition of GMD because it is the time interval necessary to release a given seismic energy content. The Arias intensity I_a [41] that considers the integral square of the ground acceleration, a measure of the energy content, is usually chosen to define this GDM. The Arias intensity is defined as:

$$I_a = \frac{\pi}{2g}\int_0^{T_t} \ddot{x}_g^2(t)dt \tag{3}$$

where $\ddot{x}_g(t)$ is the time history of the ground acceleration, g is the acceleration of gravity and T_t is the GMD of the record. The time intervals $T_{5\text{-}75}$ and $T_{5\text{-}95}$ between 5–75% and 5–95% of the Arias intensity (I_a) are respectively the two measures of significant duration most used in literature.

In this study, in order to analyze the influence of GMD on DRF, $T_{5\text{-}95}$ is considered, as it is one of the most common measure of GMD and it can be related to magnitude, distance and soil type. Different empirical formulation have been proposed in literature for effective duration [42–45] which consider the dependence on magnitude, distance and soil condition. The outcome was that effective duration increases with distance, magnitude and moving from rock to soft soil. Among these three influencing parameters, soil type has a larger influence than distance.

The present research deals with the evaluation of the influence of the effective duration on DRF for different soil conditions. To develop a suitable model for this analysis, a formulation correlating the modulating function and $T_{5\text{-}95}$ (effective duration) throughout the mean value of I_a is obtained. In this way, the stochastic dynamic response can be evaluated for different GMDs, properly defining the modulation function. In order to achieve the correlation between GMD and modulation function, the two parameters α and β in Eq. (2) are obtained by an identification procedure. Introducing the time t_m in corresponding of which the modulation function exhibits its maximum value, the parameters α and β are expressed as functions of this unknown parameter through the simultaneous equations:

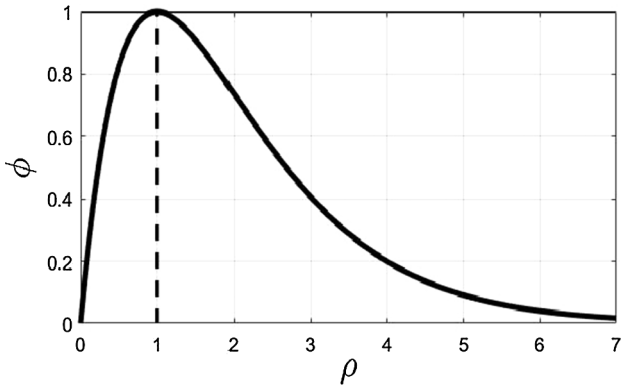

Fig. 1. Modulation function (Φ) in dimensionless time (τ).

$$\begin{cases} \phi(t_m) = 1 \\ \frac{d}{dt}\phi(t_m) = 0 \end{cases} \tag{4}$$

The two parameters α and β are then evaluated as function of t_m:

$$\beta = \frac{1}{t_m} \tag{5}$$

$$\alpha = \frac{e}{t_m} \tag{6}$$

The dimensionless time ratio $\tau = \frac{T_t}{t_m}$ can be introduced in Eq. (2), so obtaining: (see Figs. 1 and 2)

$$\phi(\tau) = \tau e^{(1-\tau)} \tag{7}$$

In order to evaluate the effective duration $T_{5\text{-}95}$, the time values at which 5% and 95% of the Arias intensity is reached can be introduced. In stochastic terms, the mean value of I_a can be evaluated as:

$$\mu[I_a] = \frac{\pi}{2g}\int_0^{T_t} \langle \ddot{x}_g^2(t)\rangle dt = \frac{\pi}{2g}\sigma_{\ddot{x}_g}^2\ \psi_a(T_t) \tag{8}$$

where T_t is the total duration of the acceleration record, $\sigma_{\ddot{x}_g}^2$ is the variance calculated for the acceleration of the ground, $\langle \ddot{x}_g^2(t)\rangle$ denotes the expected value of the square of $\ddot{x}_g$ and $\psi_a(T_t)$ is defined by:

$$\psi_a(T_t) = \int_0^{T_t} \phi^2(t)dt \tag{9}$$

Thus, using Eq. (7), Eq. (9) becomes:

$$\int_0^{\rho} \phi(\tau)^2 d\tau = \frac{1}{4}e^2(1 - e^{-2\rho}(1 + 2\rho(1 + \rho))) \tag{10}$$

where $\rho = \frac{T}{t_m}$. At the end of the phenomenon ($T = \infty$), it results:

$$\psi_a(\infty) = \int_0^{\infty} \phi(\tau)^2 d\tau = \frac{e^2}{4} \tag{11}$$

So the dimensionless time ρ_k necessary to release the k% of the total I_a is the solution of the following equation:

$$\int_0^{\rho_k} \varphi(\tau)^2 d\tau = k\int_0^{\infty} \varphi(\tau)^2 d\tau \tag{12}$$

that means in implicit form:

$$\frac{1}{4}e^2(1 - k - e^{-2\rho_k}(1 + 2\rho_k(1 + \rho_k))) = 0 \tag{13}$$

Eq. (12) allows the definition of the ρ_5 and ρ_{95} values respectively corresponding to the 5% and the 95% of the energy I_a calculated on the

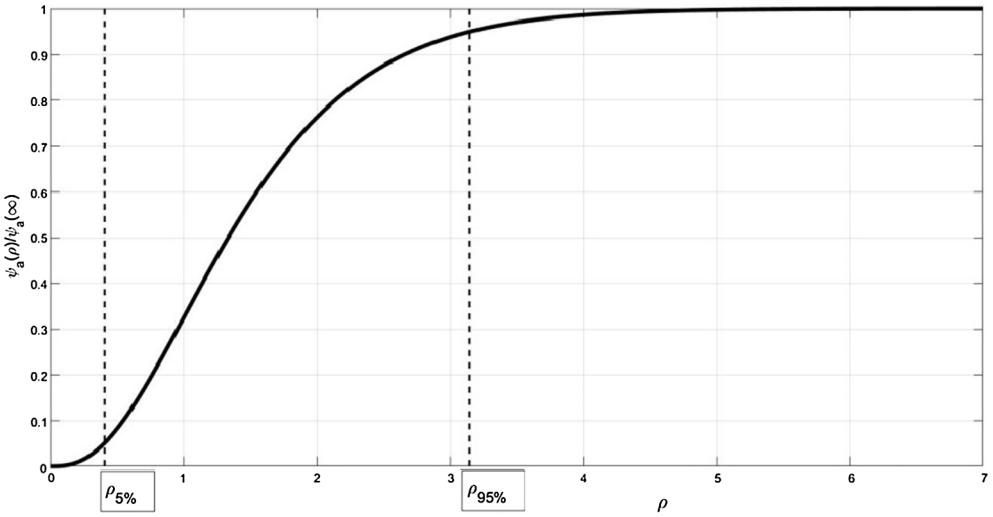

Fig. 2. $\psi_a(\rho)/\psi_a(\infty)$ in dimensionless time scale (ρ).

modulation function. The values so obtained are:

$$\rho_5 = 0.40884$$
$$\rho_{95} = 3.1478 \tag{14}$$

Thus the values t_m corresponding to the selected effective duration $T_{5\text{-}95}$ can be determined by the definition of the ratio ρ:

$$T_5 = 0.40884 t_m$$
$$T_{95} = 3.1478 t_m \tag{15}$$

Finally, the effective duration is $T_{5-95} = 2.7390 t_m$, so that it is possible to define t_m as:

$$t_m = \frac{T_{5-95}}{2.7390} \tag{16}$$

4. Evaluation of damping reduction factor by the peak theory

In this section, the seismic ground acceleration action $\ddot{X}_g(t)$ given by Eq. (1) is applied on a simple linear-viscous SDOF system to evaluate the DRF in stochastic meaning. For this system, the motion equation is:

$$\ddot{X}_s(t) + 2\xi\omega\dot{X}_s(t) + \omega^2 X_s(t) = -\ddot{X}_g(t) \tag{17}$$

where X_s is the system-ground relative displacement, ω is the natural frequency and ξ is the damping ratio:

$$\omega = \sqrt{\frac{k}{m}} \text{ and } \xi = \frac{c}{2\sqrt{km}}, \tag{18}$$

k and m being the system mass and stiffness, respectively.

In the state-space, the motion equation of the system becomes:

$$\dot{\mathbf{Z}}(t) = \mathbf{A}\mathbf{Z}(t) + \mathbf{F}(t) \tag{19}$$

where **F** is the force vector and **Z** is the state-space vector:

$$\boldsymbol{Z} = (X_s\ ,\ X_p\ ,\ X_f\ ,\ \dot{X}_s\ ,\ \dot{X}_p,\ \dot{X}_f)^T \tag{20}$$

$$\boldsymbol{F} = (0\ ,\ 0\ ,\ 0\ ,\ 0\ ,\ 0\ ,\ -\varphi(t)w(t))^T \tag{21}$$

Finally **A** is the state matrix:

$$\boldsymbol{A} = \begin{pmatrix} 0 & 0 & 0 & 1 & 0 & 0 \\ 0 & 0 & 0 & 0 & 1 & 0 \\ 0 & 0 & 0 & 0 & 0 & 1 \\ -\omega^2 & \omega_p^2 & -\omega_f^2 & -2\xi\omega & +2\omega_p\xi_p & -2\omega_f\xi_f \\ 0 & -\omega_p^2 & +\omega_f^2 & 0 & -2\omega_p\xi_p & +2\omega_f\xi_f \\ 0 & 0 & -\omega_f^2 & 0 & 0 & -2\omega_f\xi_f \end{pmatrix} \tag{22}$$

The matrix Lyapunov differential equation [46–53] can be used to calculate the stochastic response of the system when it is excited by the non-stationary modulated Clough and Penzien stochastic process:

$$\dot{\mathbf{R}}(t) = \mathrm{AR}(t) + \mathrm{R}(t)\mathrm{A}^T + \mathrm{B}(t) \tag{23}$$

where $\mathrm{R}(t) = \langle \mathrm{ZZ}^T \rangle$ is the covariance matrix and $\mathbf{B}(t)$ is a matrix that is square and has all elements equal to zero except for the last one that assumes the value $2\pi S_0 \phi(t)^2$.

For the analyzed system, a definition of the displacement spectrum is:

$$S_d = |X_s(t)|_{max} \tag{24}$$

The DRF (η) parameter permits to approximate the high damped elastic response spectrum (S_d) starting from the 5% damped one ($S_{d,\xi=5\%}$):

$$S_d = \eta S_{d,\xi=5\%} \tag{25}$$

where ξ is the damping ratio that is greater than 5% for the high damped system.

A seismic response spectrum gives the maximum displacement or acceleration response of a SDOF system when a recorded earthquake [4,6,54–60] is applied as a function of the natural period of the system. Different relations are obtained for different values of structural damping. From a stochastic point of view, the response spectrum is still a relation between the maximum acceleration or displacement response of a SDOF system, that is subjected to a ground motion, and the natural period of the SDOF system, but the maximum response and the ground motion are considered in stochastic terms. Different values of structural damping again give different response spectra.

In the present paper, the authors propose a procedure to calculate the DRF value starting from the definition of the stochastic displacement spectrum by mean of the peak theory. This theory assumes that the maximum response of a SDOF system in displacement $X_s^{\max}$ is the displacement value that is not overrun with a fixed value of the probability P_f^*. For this reason the analysis focuses on the evaluation of this maximum displacement that, from a mathematical formulation, is the displacement threshold b that will not be exceeded with a probability P_f^* during the system lifetime [61]. If this problem is analyzed for a generic process X and for a threshold b, the Vanmarcke formula [62] gives the probability that the process X exceeds the threshold b:

$$P(t, b) = 1 - \exp\left(-\int_0^t \alpha(\tau)d\tau\right) \tag{26}$$

where the expected decay rate $\alpha(\tau)$ is:

$$\alpha(\tau) = \nu_X(b,t)\frac{1-\exp\left[-\frac{\nu_R^+(b,t)}{\nu_X(b,t)}\right]}{1-\frac{\nu_X^+(b,t)}{\nu_X^+(0,t)}} \tag{27}$$

$\nu_X(b,t) = \nu_X^+(b,t) + \nu_X^-(b,t)$ being the expected rate of the response that exceeds the threshold. The up and down crossing expected rates are given by [63]:

$$\nu_X^+(b,t) = \int_{\dot b}^{\infty}(\dot x - \dot b) f_{X\dot X}(t,b;t,\dot x)d\dot x$$
$$\nu_X^-(b,t) = \int_{-\infty}^{\dot b}(\dot b - \dot x) f_{X\dot X}(t,-b;t,\dot x)d\dot x \tag{28}$$

where $f_{X\dot X}(t,b;t,\dot x)$ is the joint probability density function (JPDF) of X and $\dot X$.

In Eq. (14) the expected up-crossing rate of the envelope process $R(t)$ is indicated with $\nu_R^+(b,t)$ and $R(t)$ can be expressed as:

$$R(t) = \sqrt{X(t)^2 + \hat X^2(t)} \tag{29}$$

In Eq. (27) $\nu_R^+(b,t)$ is obtained from Eq. (15) replacing $\dot x$ and $f_{X\dot X}(t,b;t,\dot x)$ with $\dot r$ and $f_{R\dot R}(t,r;t,\dot r)$ respectively, if the JPDF $f_{R\dot R}(t,r;t,\dot r)$ is available.

For convenience, the above crossing rates are evaluated in a normalized way by introducing the normalized variables:

$$Y(t) = \frac{X(t)}{\sigma_x(t)} \tag{30}$$

$$Q(t) = \sqrt{Y(t) + \hat Y^2(t)} = \frac{R(t)}{\sigma_x(t)}\kappa(t) = \frac{b}{\sigma_x(t)} \tag{31}$$

$\sigma_x(t)$ being the standard deviation of X process and $\hat Y(t)$ the Hilbert transform of Y(t).

Since $\hat Y(t)$ and Y(t) result uncorrelated, Eqs. (15) become:

$$\nu_X^+(t,b) = \nu_Y^+(t,\kappa) = \omega_0\phi(\kappa)\left[\phi\left(\frac{\dot\kappa}{\omega_0}\right) - \frac{\dot\kappa}{\omega_0}\Phi\left(-\frac{\dot\kappa}{\omega_0}\right)\right] \tag{32}$$

$$\nu_X^-(t,b) = \nu_Y^-(t,\kappa) = \omega_0\phi(\kappa)\left[\phi\left(\frac{\dot\kappa}{\omega_0}\right) + \frac{\dot\kappa}{\omega_0}\Phi\left(-\frac{\dot\kappa}{\omega_0}\right)\right] \tag{33}$$

where ϕ is the standard normal density function, Φ is the standard normal distribution function and ω_0 is the standard deviation of $\dot Y(t)$, given by:

$$\omega_0^2 = E[\dot Y^2(t)] = E\left[\frac{\sigma_X(t)\dot X(t) - X(t)\dot\sigma_X(t)}{\sigma_X^2(t)}\right]$$
$$= \frac{\sigma_{\dot X}(t)}{\sigma_X^2(t)} - 2\frac{\dot\sigma_X(t)}{\sigma_X^3(t)}c_{X\dot X}(t) + \frac{\dot\sigma_X^2(t)}{\sigma_X^2(t)} \tag{34}$$

The functions $Q(t)$ and $\dot Q(t)$ are mutually independent in the case of a normal process, with the Rayleigh and normal distribution respectively given by:

$$f_Q(q) = q\exp\left(-\frac{q^2}{2}\right) \tag{35}$$

$$f_{\dot Q}(\dot q) = \frac{2}{\sqrt{2\pi(\omega_0^2 - \lambda^2)}}\exp\left(-\frac{1}{2}\frac{\dot q^2}{(\omega_0^2 - \lambda^2)}\right) \tag{36}$$

where $\lambda(t)$ is the covariance of $Y(t)$ and $\hat{\dot Y}(t)$. Since X(t) and $\hat X(t)$ are uncorrelated, $\hat X(t)$ and $\hat{\dot X}(t)$ are uncorrelated too. Starting from the above equations, it is simple to introduce the relation:

$$\lambda(t) = E[Y(t)\hat{\dot Y}(t)] = E\left[\frac{X(t)}{\sigma_X(t)}\frac{\sigma_X(t)\hat{\dot X}(t) - \hat X(t)\dot\sigma_X(t)}{\sigma_X^2(t)}\right] = \frac{c_{X\dot X}(t)}{\sigma_X^2(t)} \tag{37}$$

Then the evaluation of the up-crossing rate for the envelope is possible by:

$$\upsilon_R^+(t,b) = \upsilon_Q^+(t,\kappa) = f_Q(\kappa)\int_{\dot\eta}^{\infty}(s-\dot\kappa)f_{\dot Q}(s)ds =$$
$$\sqrt{\omega_0^2 - \lambda^2}\,\kappa e^{-\frac{\kappa^2}{2}}\left[\phi\left(\frac{\dot\kappa}{\sqrt{\omega_0^2-\lambda^2}}\right) - \frac{\dot\kappa}{\sqrt{\omega_0^2-\lambda^2}}\Phi\left(-\frac{\dot\kappa}{\sqrt{\omega_0^2-\lambda^2}}\right)\right] \tag{38}$$

If $\sigma_X^2(t)$, $\sigma_{\dot X}^2(t)$, $c_{X\dot X}(t)$ and $c_{X\dot{\hat X}}(t)$ are available, then the crossing rates of $X(t)$ and $R(t)$ can be evaluated directly. The variation of the natural period of the SDOF allows to calculate the displacement spectrum. $X_{\max}^{P^*}(t)$ is the maximum displacement such that the probability that $X(t)$ will exceed the domain $[-X_{\max}^P, +X_{\max}^P]$ is equal to a given value P^*. This inverse problem can be solved by a numerical approach as described in [61].

5. Analysis results

In this section, a sensitivity analysis on DRF is carried out considering the effect of natural period, damping ratio, soil type and effective duration. More in details, different effective durations are considered, and the modulation function parameters are identified by the procedure described in Section 4. A wide range of GMD are considered, in order to cover all possible earthquakes. Different soil conditions are analyzed (soft, medium and rigid) by assigning the Clough and Penzien model parameters as reported in Table 1. In the analysis it is assumed $P^* = 10^{-3}$.

Figs. 3–5 show the variability of DRF (η) for different soil conditions versus the system natural period $T_0 = 2\pi/\omega$. Each plot corresponds to an assigned value of the system damping ratio ξ. Six values of ξ are considered: 0.10, 0.15, 0.20, 0.40, 0.60 and 0.80. Vertical line defines the ground motion predominant period $T_f = 2\pi/\omega_f$. Fig. 3 shows the results for a soft soil. Different colored lines correspond to different values of the effective duration T_{5-95}, which varies in the range 10.94–54.80 sec. The dependences among the parameters damping ratio, structural vibration period, soil type and GMD are represented by means of the plots in Figs. 3–5. The DRF shows a period-dependent trend in Fig. 3. It is worth noting that all curves show the same variability as T_0 varies and moves downwards and as the damping ratio increases in the considered range. The lowest values of DRF occurs when the natural period T_0 equals the predominant period of earthquake T_f. In detail, for $T_0 < T_f$ the DRF decreases with the increase of T_0 and reaches a minimum in T_f. Then, for $T_0 > T_f$ the DRF increases with the increase of the natural period T_0. The DRF tends to assume a unity value in correspondence of the lowest or highest values of period. This can be explained by the fact that the forces can be independent from the damping ratio in a very stiff or very flexible structure. It also emerges that DRF value decreases as damping ratio ξ increases. These results have been observed by Zhou et al. [29]. In addition, when period changes the DRF variation seems lower for low damping ratio. For example for $\xi = 0.1$ (Fig. 3), DRF varies between 0.84 and 0.64 (for a GMD of 54.8 sec), whereas for $\xi = 0.8$, DRF varies between 0.57 and 0.12 (for a GMD of 54.8 sec).

With regard to the variability of DRF with GMD, that is the main topic of this study, two different considerations can be carried out: firstly, it is noticed that as the GMD increases, the DRF decreases and the plots move downwards. This variability of DRF with GMD is in agreement with the studies from Bommer et al. [21] and Zhou et al. [29]. These authors observed a decrease of DRF when GMD increases. In addition, results show a larger variability of DRF with GMD in the range of high natural periods. The results of these studies make evident that the GMD has important effects on DRF and this should be

Table 1
Filter parameters for different soil types.

Soil type	ω_p(rad/sec)	ξ_p	ω_c(rad/sec)	ξ_c
Rigid	15	0.6	1.5	0.6
Medium	10	0.4	1	0.6
Soft	5	0.2	0.5	0.6

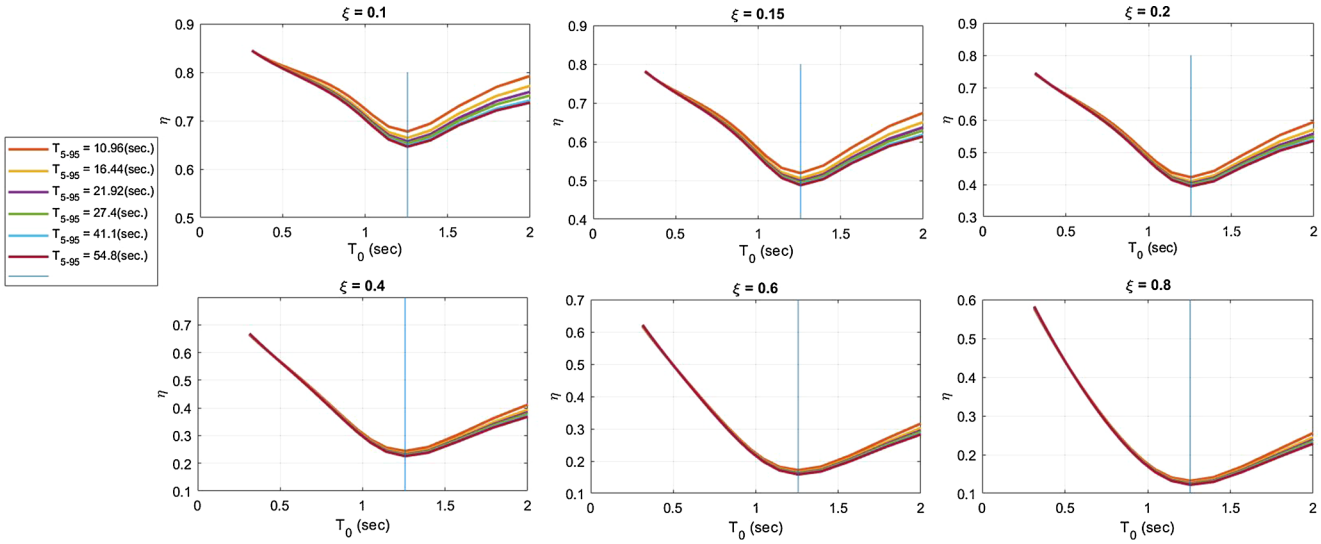

Fig. 3. Variability of DRF (η) with system natural period (T_0) for soft soil. The ground motion predominant period (T_f) is the blue line. (For interpretation of the references to color in this figure legend, the reader is referred to the web version of this article.)

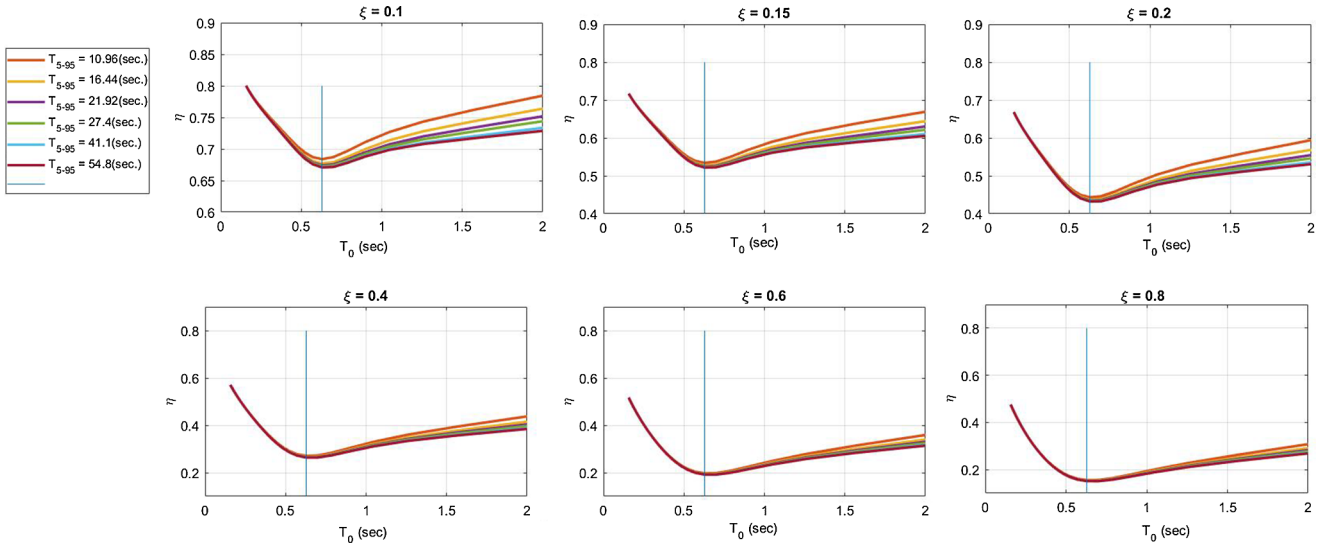

Fig. 4. Variability of DRF (η) with system natural period (T_0) for medium soil. The ground motion predominant period (T_f) is the blue line. (For interpretation of the references to color in this figure legend, the reader is referred to the web version of this article.)

considered in engineering applications. Secondly, the influence of earthquake GMD depends on damping ratio and it seems larger for systems with lower damping ratio and tends to reduce as the damping ratio increases. Later we will see that this is not always true.

Figs. 4 and 5 show the results of the sensitivity analysis for medium and rigid soils. Firstly, it is observed that the soil type affects the DRF and more precisely DRF is larger for soft soil. This result agrees with the ones presented by Lin et al. [19]: the soil type has a significant effect on DRF especially for very stiff and rock sites. The aspects related to the influence of soil type on DRF have been discussed in a previous study by the authors to which reference is made [31]. With regard to the variability of DRF with earthquake effective duration, the same variability of DRF, already observed in the case of soft soil, is observed for medium and rigid soils when GMD varies. Moreover, the dependency of DRF on effective duration is more evident in these two cases with respect to soft soil. Also for medium and rigid soil it is observed that the variability of DRF is more evident for small values of structural damping (ξ = 0.10–0.20) while tends to be negligible for greater values.

To better analyze the influence of natural period and damping ratio on the variation of DRF as a function of the effective duration, it is useful to analyze Figs. 6–8, representing the DRF (η) versus the effective duration ($T_{5\text{-}95}$). Different colored[1] lines correspond to different values of system damping ratio (ξ); the 4 sub-figures correspond to different system natural periods T_0 ($T_0 = 0.5$ sec, $T_0 = 1$ sec, $T_0 = 1.5$ sec, $T_0 = 2$ sec).

Firstly, the case of soft soil is analyzed. It is observed that earthquake GMD does not affect the DRF for system with low natural period ($T_0 = 0.5$ sec), except for earthquakes with a very short duration. If an exception is made for the curve corresponding to the lowest value of the damping ratio $\xi = 0.10$, the curves are practically horizontal. When the natural periods of the system increase, a greater influence of the GMD on the DRF is observed, even for high values of damping ratio. The largest effects of the GMDs are for the system with natural period

[1] For interpretation of color in Figs. 6–8 and 12, the reader is referred to the web version of this article.

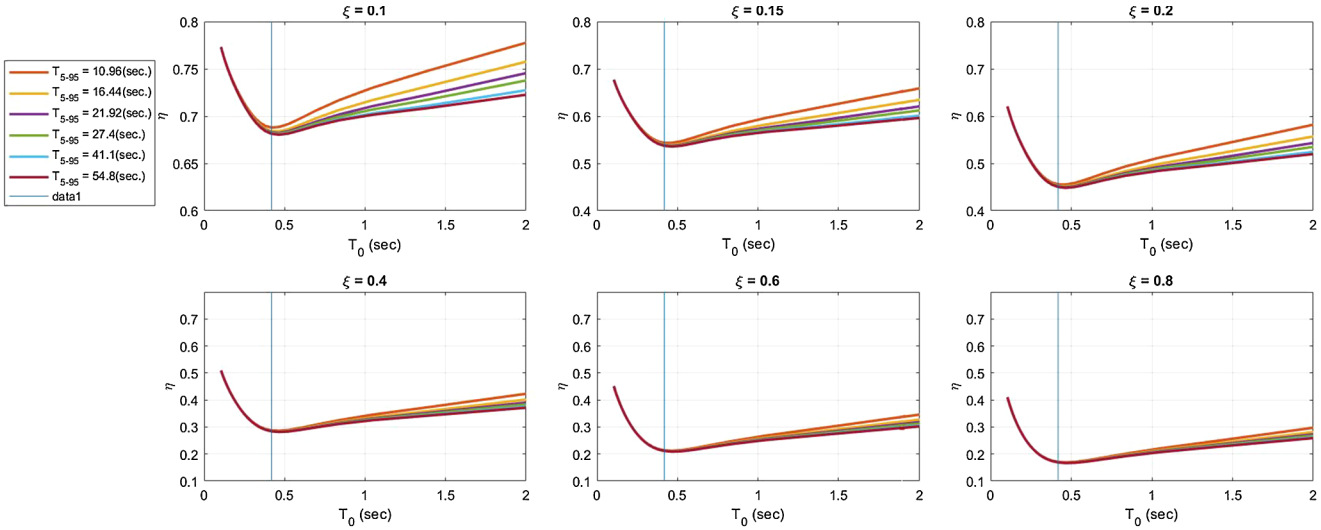

Fig. 5. Variability of DRF (η) with system natural period (T_0) for rigid soil. The ground motion predominant period (T_f) is the blue line. (For interpretation of the references to color in this figure legend, the reader is referred to the web version of this article.)

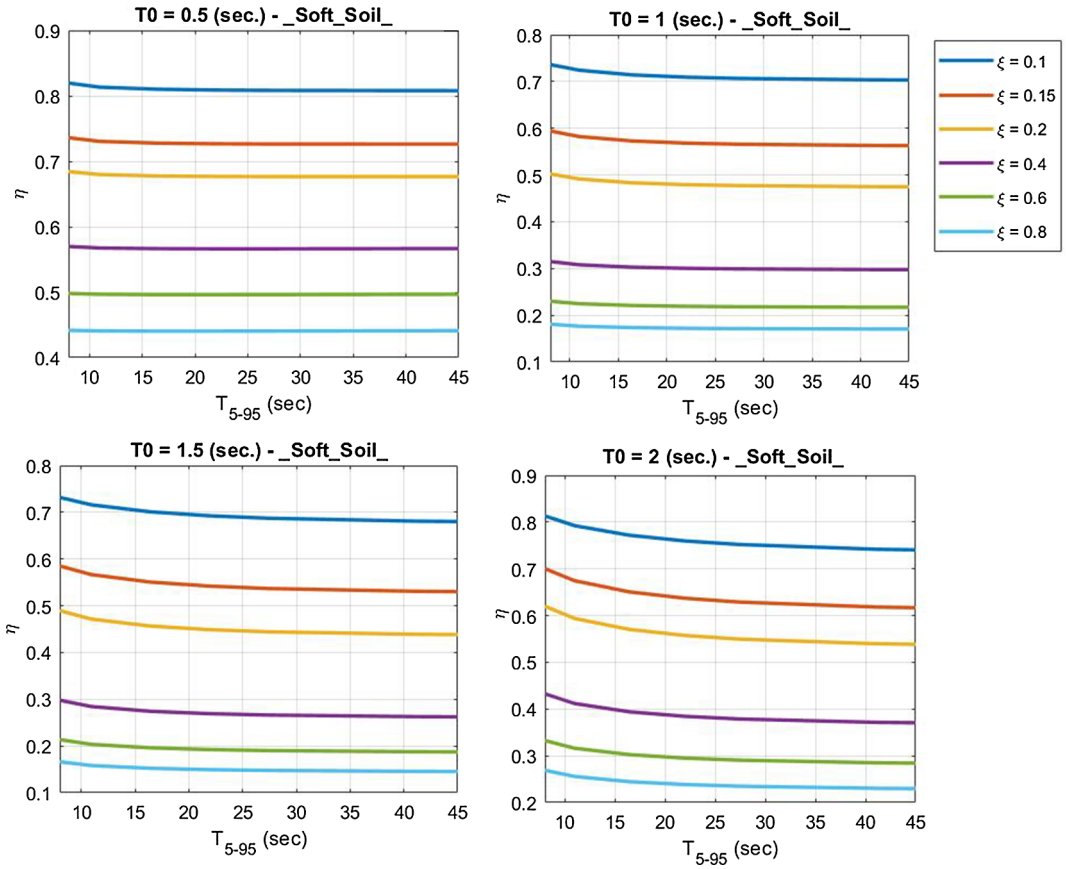

Fig. 6. Variability of DRF (η) with earthquake effective duration ($T_{5\text{-}95}$) for soft soil; T_0 is the system natural period.

T = 2 sec. In this case, the DRF varies between 0.82 and 0.72 (values evaluated for $\xi = 0.10$). This variability is important since it leads to a 12% reduction of the spectral response and the implications in practical engineering applications are relevant. As before mentioned, a greater GMD value means a greater time window in which the seismic recording is analyzed. If the GMD increases, the number of cycles of the seismic event increases and so also damping effects on the response of the system increase. Consequently this produces [64] the decrease of DRF value. By observing in detail plots in Figs. 6–8, it emerges that DRF variation with GMD is significant in the initial part, while successively it reaches gradually a steady state. Generally, it is observed that for a GMD greater than 20 sec the GMD of the excitation does not affect DRF. This result agrees with Stafford et al. [65]. This outcome is also consistent with the conclusions from Zhou et al [29]. The authors concluded that the maximum displacement curve shows a plateau without increasing further in the case of a system on which a higher number of cycles is applied. This study is based on the analysis of the harmonic excitation of SDOF and the results show that DRF is almost constant for

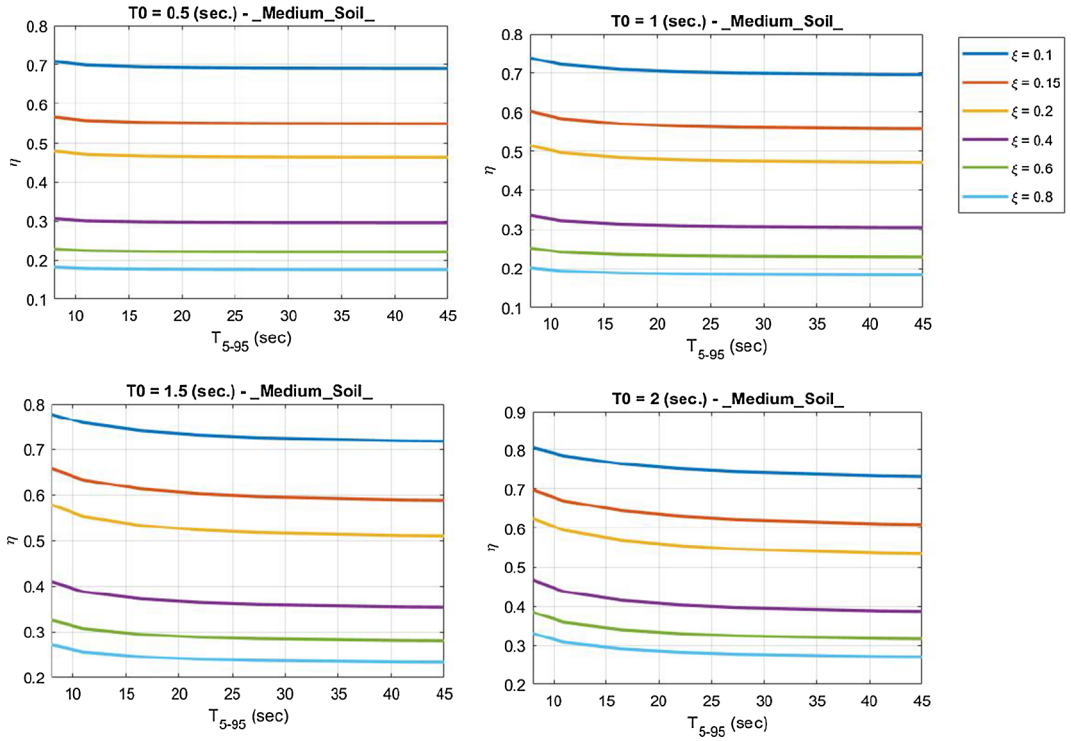

Fig. 7. Variability of DRF (η) with earthquake effective duration ($T_{5\text{-}95}$) for medium soil; T_0 is the system natural period.

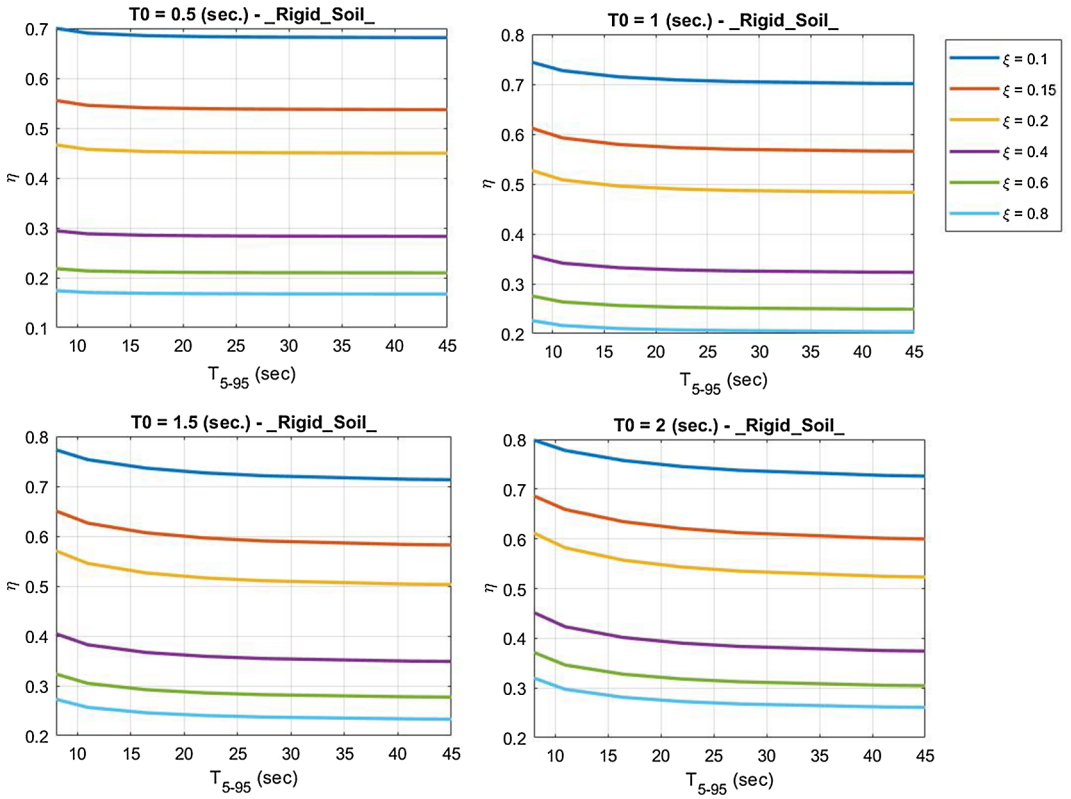

Fig. 8. Variability of DRF (η) with earthquake effective duration ($T_{5\text{-}95}$) for rigid soil; T_0 is the system natural period.

each damping value. In addition, at all damping ratio values, the variation trends of DRF with the effective duration result consistent with each other.

The greatest variability of DRF is observed for $T_0 = 2$ sec. The same considerations can be made by observing the graphs in Figs. 7 and 8, which refer to a medium and rigid soil, respectively. As already mentioned, for this last type of soil the greater variability of DRF with the earthquake GMD can be observed.

In order to evaluate the amount of the DRF variation with GMD in Figs. 9–11 the maximum variability of DRF ($\Delta(\eta)$), that is the DRF value

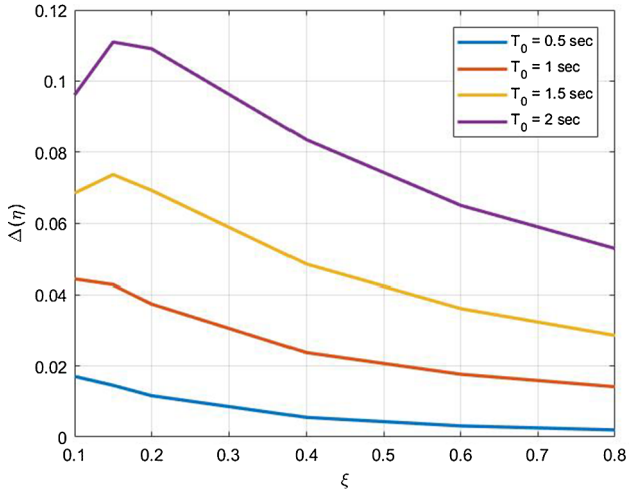

Fig. 9. Maximum variability of DRF (Δ(η)) with system damping ratio for soft soil; T_0 is the system natural period.

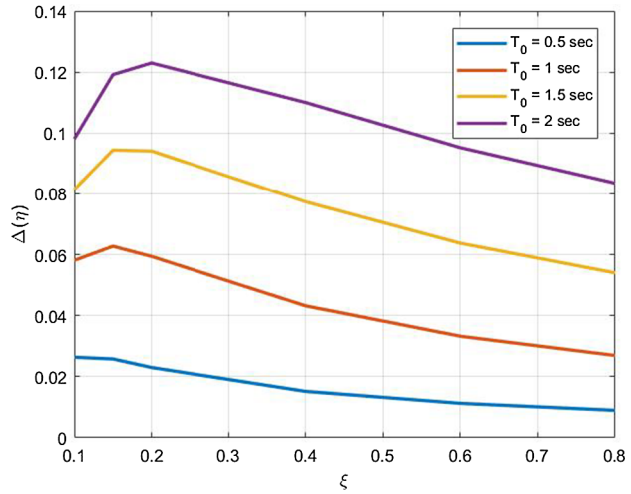

Fig. 10. Maximum variability of DRF (Δ(η)) with system damping ratio for medium soil; T_0 is the system natural period.

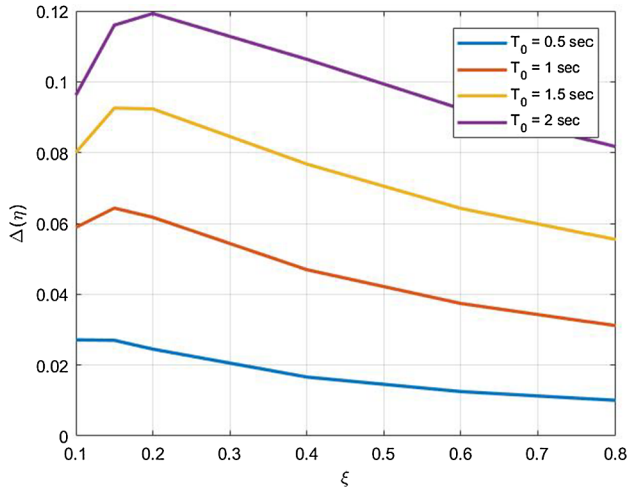

Fig. 11. Maximum variability of DRF (Δ(η)) with system damping ratio for rigid soil; T_0 is the system natural period.

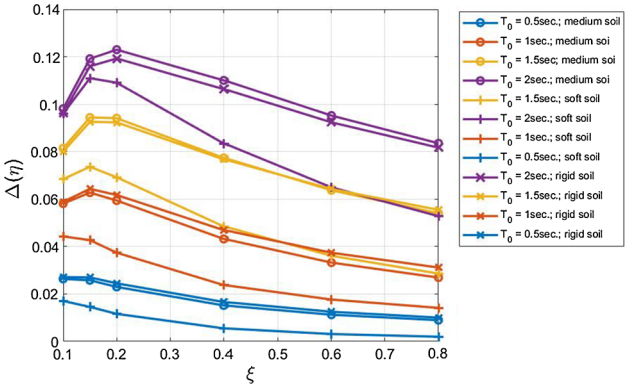

Fig. 12. Comparison of maximum variability of DRF (Δ(η)) with system damping ratio for different soils; T_0 is the system natural period.

evaluated for the lower effective duration minus the DRF value evaluated for the larger effective duration, is shown. All soil conditions are considered. From Fig. 9 (soft soil), it can be firstly observed that the influence of the effective duration on DRF is more relevant in the range of high periods. The maximum variation equal to 0.11 is for $T_0 = 2$ sec and $\xi = 0.15$. For $T_0 = 0.5$ sec the variability of DRF with effective duration always decreases as the damping ratio increases, whereas as the system becomes more deformable a different behavior can be observed. In fact, as the damping ratio increases, the effect of effective duration on DRF firstly increases and then decreases as the damping ratio grows up. This tendency is more evident for the system with the largest natural period considered in this study ($T_0 = 2$ sec). From Figs. 10 and 11 (medium and rigid soil) an analogous behavior can be observed.

Fig. 12 shows the maximum DRF variability $\Delta\eta(\eta)$ as damping ratio increases. The different colored lines correspond to the 4 structural periods analyzed, while the three symbols on the curves identify the three soil types. The variability of DRF with GMD is influenced by the natural periods of the system, by the damping ratio and by the soil type. The greater variability is for deformable systems on rigid soils and generally in the range of low damping ratio values, although a precise damping value at which the maximum variability is obtained can be identified. For rigid soil, the maximum DRF variability $\Delta\eta(\eta)$ is 0.125 for $\xi = 0.2$.

6. Proposed DRF formulation

In this section a novel formulation for the DRF useful for practical application, which, in addition to period and damping, also accounts for the effects of GMD and soil characteristics, is furnished:

$$DRF(\xi,\ T_0,\ T_{5-95}) = \left(\frac{1 + \psi(T_0)\left(\frac{T_{5-95}}{T_0}\right)\xi}{1 + \psi(T_0)\left(\frac{T_{5-95}}{T_0}\right)0.05} \right)^{\vartheta(T_0)} \tag{39}$$

where

$$\psi(T_0) = \alpha e^{-\beta T_0} \tag{40}$$

$$\vartheta(T_0) = \chi + \delta T_0 \tag{41}$$

Table 2
Parameters in Eqs. (40) and (41) for different soil types.

Soil type	α	β	χ	δ
Rigid	16.3450	0.4626	0.4626	−0.6286
Medium	18.9182	0.5615	0.0677	−0.6259
Soft	171.8278	2.0195	−0.1364	−0.3302

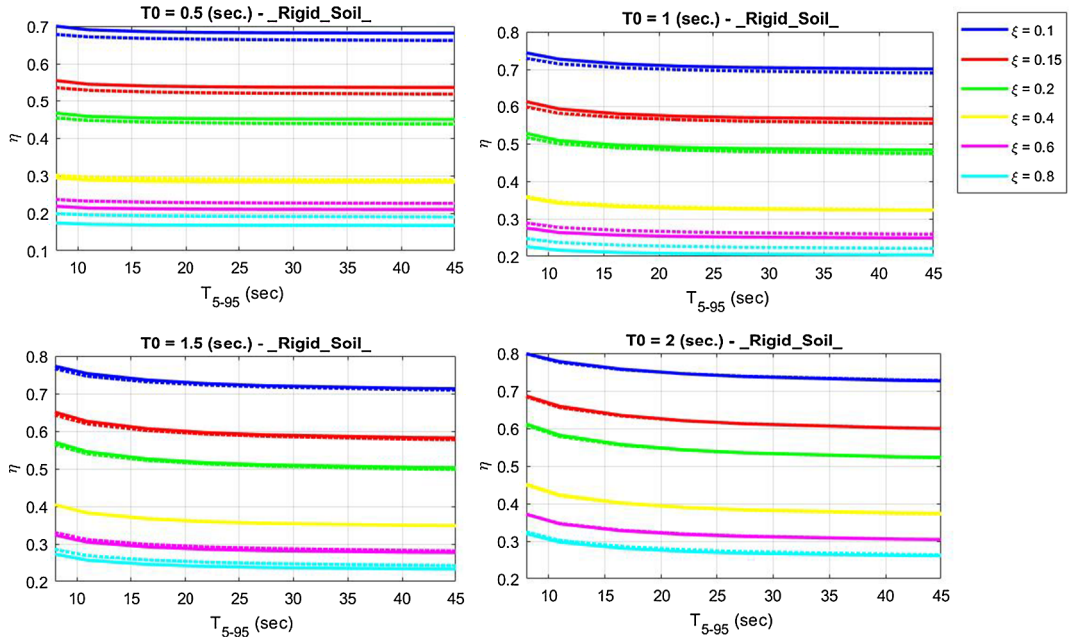

Fig. 13. Comparison between the proposed formulation (Dashed line) and the results from stochastic analysis (continuous line) for DRF (η) in case of rigid soil; ξ is the damping ratio.

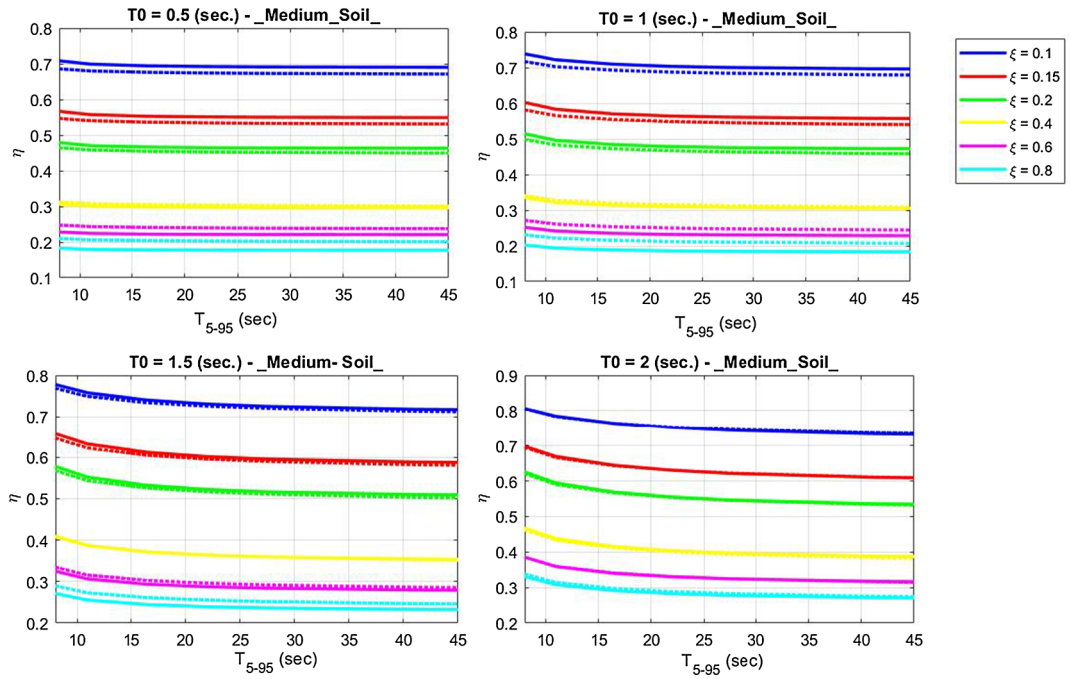

Fig. 14. Comparison between the proposed formulation (Dashed line) and the results from stochastic analysis (continuous line) for DRF (η) in case of medium soil; ξ is the damping ratio.

Nonlinear multiple regressions are carried out by using a Matlab code [66,67] to acquire the relationship that assures the best-fit of DRF, accounting for the influence of the soil type, GMD, damping ratio and natural period. The parameters in Eqs. (40) and (41) are given in Table 2.

In order to assess the efficiency of the developed regression, firstly a comparison with the results deriving from the stochastic analysis is shown. Figs. 13–15 show the comparison between the proposed formulation and the results from the stochastic analysis for different soils. The dashed line is the proposed formulation while the continuous line is the result obtained by the stochastic analysis. A very good agreement is noticeable for rigid soil and medium soil whereas for soft soil some discrepancies can be observed in the range of high natural periods. For rigid soil, except for $T_0 = 0.5$ sec, the curves are practically coincident each other.

Finally, it would be interesting to compare the proposed formulation with results performed by other studies. However as explained in the introduction, there are not studies which simultaneously consider the effect of soil type and GMD on DRF. Therefore, a possibility is to compare the results attained by the proposed formulation with the results reported in [68], in which only the influence of damping ratio, natural period and duration, but not of soil type, is considered.

The results of this comparison are shown for different soils in Figs. 16–18. The comparison outlines that in some cases the Zhou's

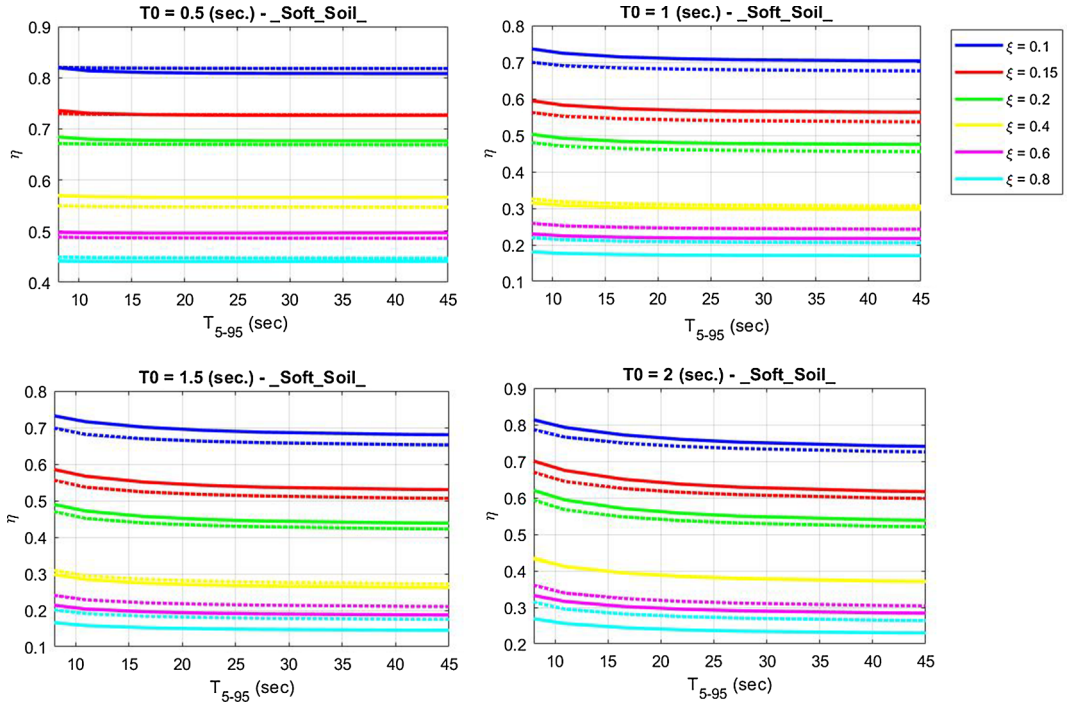

Fig. 15. Comparison between proposed formulation (Dashed line) and results from stochastic analysis (continuous line) for DRF (η) in case of soft soil; ξ is the damping ratio.

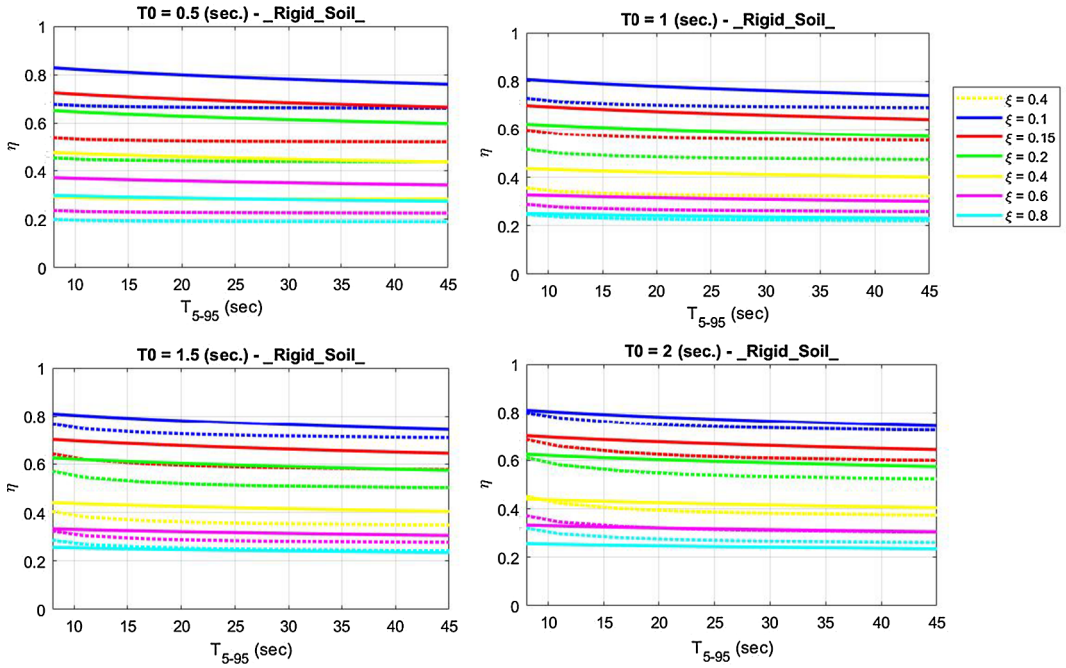

Fig. 16. Comparison between proposed formulation (Dashed line) and results in [68] in case of rigid soil; ξ is the damping ratio.

formula overestimates the value of the DRF compared to the proposed formulation. This is generally true for low natural periods and for low damping. The proposed formulations, on the contrary, are in good agreement for $T_0 = 2.0$ sec and for high damping ratio.

The results obtained from this work have a practical relevance in seismic engineering applications as they allow a more accurate evaluation of DRF, accounting also for soil type influence, differently from other formulation existing in literature. One should remind that, in practical cases, the effective GMD can be evaluated by existing formulations [69] for a given earthquake scenario, identified by parameters such as magnitude, epicentral distance and soil type, and therefore the DRF factor could be calculated by applying the proposed formulation for a particular value of damping at any specific period of the structure.

7. Conclusion and further developments

In this study, a combined evaluation of DRF sensitivity to ground

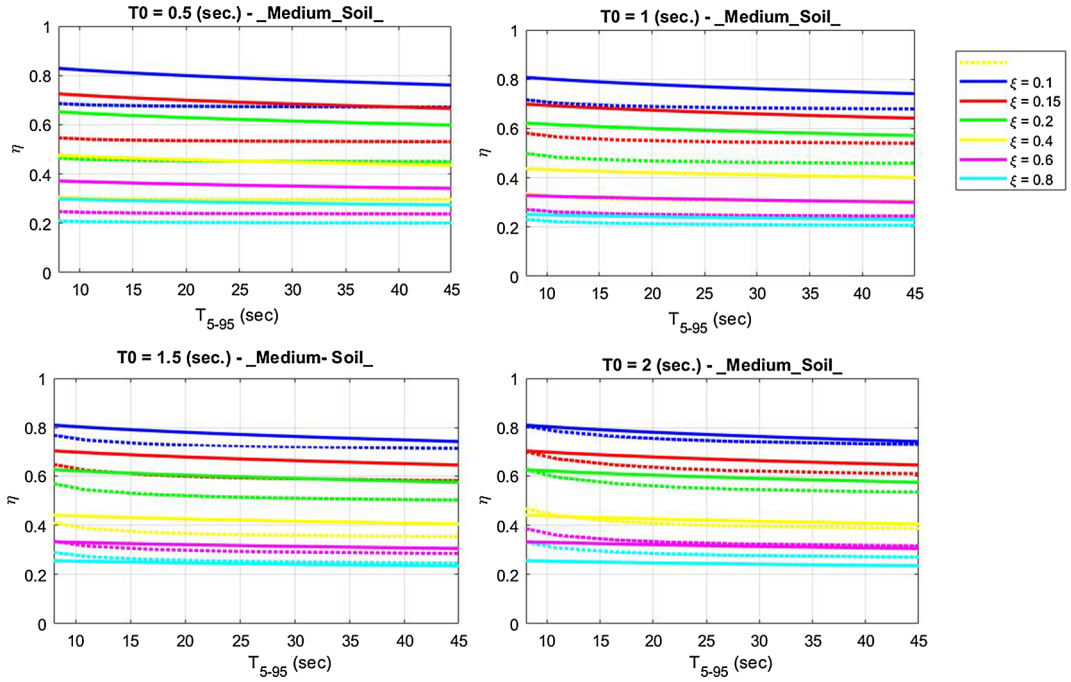

Fig. 17. Comparison between proposed formulation (Dashed line) and results in [68] in case of medium soil; ξ is the damping ratio.

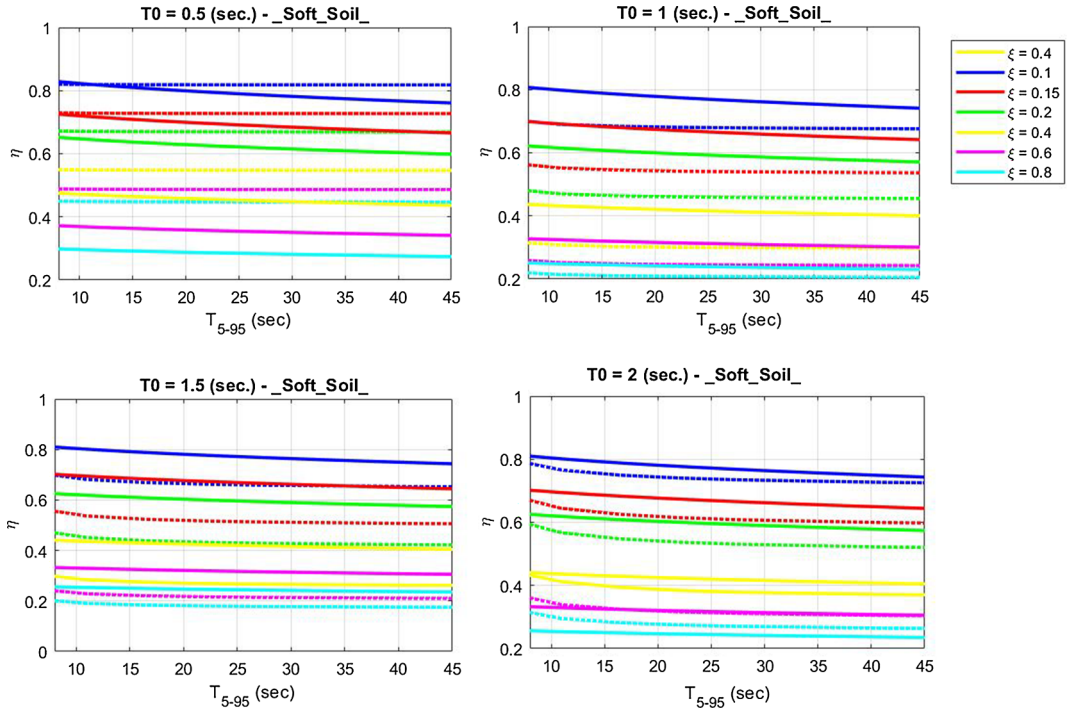

Fig. 18. Comparison between proposed formulation (Dashed line) and results in [68] in case of soft soil.

motion duration (GMD), soil type, damping ratio and natural period has been studied; the peak theory of stochastic processes is at the base of the proposed procedure. This theory models seismic excitation by a non-stationary process defined by means of a stationary predominant frequency and a given bandwidth. The parameters of the modulation function have been chosen in order to represent earthquakes with different effective durations. The following conclusions can be given on the base of the obtained results. Firstly, the research results are in agreement with previous studies with concerning the influence of damping ratio on DRF: in detail DRF decreases with the increase of damping ratio. Moreover, DRF is significantly dependent on the vibration period, reaching its minimum value in correspondence of a natural period equal to the earthquake predominant one.

Secondly, the effective duration influences DRF: as effective duration increases, DRF decreases. However, this variability is evident in the first part of the effective GMD, for reaching the steady state response in the final part. For GMDs larger than 20 sec, the DRF tends to an asymptotic final value and there are no significant differences among

them (the same result for different GMDs). However, this sensibility especially concerns deformable systems (in the study $T_0 = 2$ sec is considered) with low damping ratio and becomes negligible for rigid structures ($T_0 = 2$) with high damping ratio. In addition, this sensitivity results greater for small damping ratios ($\xi = 0.10$) and reduces as the damping ratio increases. The DRF also depends on ground type and a larger sensitivity is observed for rigid soil. For example, for this soil, the variation of DRF can amount to 0.125 and the implication on practical applications can be relevant.

Based on the conducted stochastic analyses, a simple formulation for DRF evaluation, accounting for effective duration, soil type, damping ratio and natural period, has finally been given.

This study gives results with great relevance in structural applications since it shows that earthquake GMD should be considered not only for damage structural assessment but also for DRF evaluation in order to avoid an underestimation of structural seismic forces. This aspect is more relevant for deformable structures on rigid soil and with low damping ratio. Therefore the proposed formulation of DRF, also accounting for the effects of GMD and soil characteristics in addition to period and damping, results particularly useful for practical applications.

Appendix A. Supplementary material

Supplementary data to this article can be found online at https://doi.org/10.1016/j.engstruct.2018.10.074.

References

[1] Fiorentino G, Forte A, Pagano E, Sabetta F, Baggio C, Lavorato D, et al. Damage patterns in the town of Amatrice after August 24th 2016 central Italy earthquakes. Bull Earthq Eng 2018;16(3):1399–423.
[2] Nuti C, Santini S, Vanzi I. Damage, vulnerability and retrofitting strategies for the Molise hospital system following the 2002 Molise, Italy. Earthq Earthq Spectra 2004;20(S1):S285–99.
[3] Rasulo A, Goretti A, Nuti C. Performance of lifelines during the 2002 Molise, Italy. Earthq Earthq Spectra 2004;20(S1):S301–14.
[4] Nuti C, Rasulo A, Vanzi I. Seismic assessment of utility systems: application to water, electric power and transportation networks. In: Safety, reliability and risk analysis: theory, methods and applications - proceedings of the joint ESREL and SRA-Europe conference, vol. 3; 2009. p. 2519–29.
[5] Bergami AV, Nuti C. A design procedure of dissipative braces for seismic upgrading structures. Earthq Struct 2013;4(1):85–108.
[6] Lavorato D, Vanzi I, Nuti C, Monti G. Generation of non-synchronous earthquake signals. In: Gardoni P, editor. Springer series in reliability engineering. Cham: Springer International Publishing; 2017. p. 169–98.
[7] Liu T, Zordan T, Zhang Q, Briseghella B. Equivalent viscous damping of bilinear hysteretic oscillators. J Struct Eng 2015;141(11):06015002.
[8] Lin YY, Miranda E, Chang KC. Evaluation of damping reduction factors for estimating elastic response of structures with high damping. Earthq Engrg Struct Dyn. 2005;34:1427–43.
[9] NEHRP. Recomended provisions for seismic regulations for new buildings and other structures. Washington, DC: Federal Emergency Management Agency; 2000.
[10] UBC. Uniform Building Code. Whittier, CA: International Conference of Building Officials; 1997.
[11] FEMA-273. NEHRP guidelines for the seismic rehabilitation of buildings. Washington DC: Fed.Emergency Management Agency; 1997.
[12] IBC. International Building Code. Whittier, CA: International Conference of Building Officials; 2000.
[13] Fiore A, Marano GC, Natale MG. Theoretical prediction of the dynamic behavior of rolling-ball rubber-layer isolation systems. Struct Control Health Monit 2016;23(9):1150–67.
[14] Marano GC, Pelliciari M, Cuoghi T, Briseghella B, Lavorato D, Tarantino AM. Degrading bouc-wen model parameters identification under cyclic load. Int J Geotech Earthq Eng 2017;8(2):60–81.
[15] Marano GC, Pelliciari M, Cuoghi T, Briseghella B, Lavorato D, Tarantino AM. Parameter identification of degrading and pinched hysteretic systems using a modified Bouc-Wen model. Struct Infrastruct Eng 2018.
[16] Ashour SA. Elastic seismic response of buildings with supplemental damping PhD. Thesis Department of Civil Engineering, Michigan University; 1987.
[17] Ramirez OM, Constantinou MC, Whittaker AS, Kircher CA, Chrysostomou CZ. Elastic and inelastic seismic response of buildings with damping systems. Earthq Spectra 2002;18(3):531–47.
[18] Bommer JJ, Elnashai AS, Weir AG. Compatible acceleration and displacement spectra for seismic design codes. In: Proceedings of the 12th world conference on earthquake engineering, Auckland; 2000.
[19] Lin YY, Chang KC. A study on damping reduction factor for buildings under earthquake ground motion. J Struct Eng 2003;129(2):206–14.
[20] Lin YY, Chang KC. Effects of site classes on damping reduction factors. J Struct Eng 2004;130(11):1667–75.
[21] Bommer JJ, Mendis R. Scaling of spectral displacement ordinates with damping ratios. Earthq Eng Struct Dynam 2005;34:145–65.
[22] Cameron WI, Green RA. Damping correction factors for horizontal ground motion response spectra. Bull Seismol Soc Am 2007;97(3):934–60.
[23] Akkar S, Sandıkkaya MA, Ay BÖ. Compatible ground-motion prediction equations for damping scaling factors and vertical-to-horizontal spectral amplitude ratios for the broader Europe region. Bull Earthq Eng 2014;1(12):517–47.
[24] Benahemd B, Hamoutenne M, Tiliouine B, Badaoui M. Prediction of the damping reduction factor by neural networks. Asian J Civil Eng (BHRC) 2016;17:225–34.
[25] Stafford PJ, Mendis R, Bommer JJ. Dependence of damping correction factors for response spectra on duration and numbers of cycles. J Struct Eng 2008;8:1364–73.
[26] Rosenblueth E. Characteristics of earthquakes. In: Rosenblueth E, editor. Design of Earthquake Resistant Structures. Wiley; 1980 Chapter 1.
[27] Anbazhagan P, Neaz Sheikh M, Bajaj Ketan, Mariya Dayana PJ, Madhura H, Reddy GR. Empirical models for the prediction of ground motion duration for intraplate earthquakes. J Seismol 2017;21:1001.
[28] Daneshvar P, Bouaanani N, Goda K, Atkinson GM. Damping reduction factors for crustal, inslab, and interface earthquakes characterizing seismic hazard in Southwestern British Columbia, Canada. Earthq Spectra 2016;32:45–74.
[29] Zhou J, Tang K, Wang H, Fang X. Influence of ground motion duration on damping reduction factor. J Earthq Eng 2014;18:816–30.
[30] Rezaeian S, Bozorgnia Y, Idriss IM, Campbell K, Abrahamson N, Silva W. Damping scaling factors for elastic response spectra for shallow crustal earthquakes in active tectonic regions: average horizontal component. Earthq Spectra 2014.
[31] Greco R, Fiore A, Briseghella B. Influence of soil type on damping reduction factor: a stochastic analysis based on peak theory. Soil Dyn Earthq Eng 2018;104:365–8.
[32] Greco R, Fiore A, Marano GC. The role of modulation function in nonstationary stochastic earthquake model. J Earthq Tsunami 2014;8(5):1450015-1–1450015-28.
[33] Greco R, Marano GC, Fiore A. Performance-cost optimization of tuned mass damper under low-moderate seismic actions. Struct Des Tall Special Build 2016;25(18):1103–22.
[34] Marano GC. Envelope process statistics for linear dynamic system subject to non-stationary random vibrations. Far East J Theor Stat 2008;26:29–46.
[35] Clough WR, Penzien J. Dynamics of Structures. McGraw-Hill Education (ISE Editions); International 2 Revised ediction (dicember 1993); 1977.
[36] Jennings PC, Housner GW, Tsai NC. Simulated earthquake motions. Technical report, Earthquake Engnrg. Res. Lab., California Inst. of Technology; 1968.
[37] Bommer JJ, Martinez-Pereira A. The effective duration of earthquake strong motion. J Earthq Eng 1999;3:127–72.
[38] Bolt BA. Duration of strong ground motions. In: Proceedings of the 5th world conference on earthquake engineering, Acapulco; 1973.
[39] Sabetta F. Analisi di quattro definizioni di durata applicate ad accelerogrammi relativi a terremoti italiani. Open File Report, ENEA -RT/AMB 4(83), Roma, Italy; 1983 [Italian].
[40] Sarma SK, Casey BJ. Duration of strong motion in earthquakes. In: Proceedings of the 9th European Conference on Earthquake Engineering, Moscow, USSR, 10A. 1990; p. 174–83.
[41] Arias A. A measure of earthquake intensity. Hansen RJ, editor. Seismic design for nuclear power plants, vol. 23. Cambridge, Massachusetts: MIT Press; 1970. p. 438–83.
[42] Trifunac MD, Brady AG. A study on the duration of strong earthquake ground motion. Bull Seismol Soc Am 1975;65:581–626.
[43] Bommer JJ, Stafford PJ, Alarcon JA. Empirical equations for the prediction of the significant, bracketed, and uniform duration of earthquake ground motion. Bull Seismol Soc Am 2009;99(6):3217–33.
[44] Kempton JJ, Stewart PJ. Prediction equations for significant duration of earthquake ground motions consideration site and near- source effects. Earthq Spectra 2006;22:958–1013.
[45] Hernandez B, Cotton F. Empirical determination of the ground shaking duration due to an earthquake using strong motion accelerograms for engineering applications. In: Proceedings, 12th world conference on earthquake engineering. 2000; paper no. 2254/4/A.
[46] Lutes LD, Sarkani S. Failure analysis. Random vibrations. London: Butterworth-Heinemann; 2004. p. 500–70 Chapter 11.
[47] Marano GC, Acciani G, Fiore A, Abrescia A. Integration algorithm for covariance non-stationary dynamic analysis of SDOF systems using equivalent stochastic linearization. Int J Struct Stab Dyn 2015;15(2):1450044-1–1450044-17.
[48] Greco R, Marano GC, Fiore A. Damage-based inelastic seismic spectra. Int J Struct Stab Dyn 2017;17(10):1750115-1–1750115-23.
[49] Marano GC, Trentadue F, Greco R. Stochastic optimum design criterion of added viscous dampers for buildings seismic protection. Struct Eng Mech 2007;25(1):21–37.
[50] Greco R, Marano GC. Optimum design of tuned mass dampers by displacement and energy perspectives. Soil Dyn Earthq Eng 2013;49:243–53.
[51] Lucchini A, Greco R, Marano GC, Monti G. Robust design of tuned mass damper systems for seismic protection of multistory buildings. J Struct Eng 2014;140(8):A4014009.
[52] Greco R, Lucchini A, Marano GC. Robust design of tuned mass dampers installed on multi-degree-of-freedom structures subjected to seismic action. Eng Optim 2015;47(8):1009–30.
[53] Marano GC, Trentadue F, Greco R. Optimum design criteria for elastic structures subject to random dynamic loads. Eng Optim 2006;38(7):853–71.
[54] Vanzi I, Marano GC, Monti G, Nuti C. A synthetic formulation for the Italian seismic

hazard and code implications for the seismic risk. Soil Dyn Earthq Eng 2015;77:111–22.
[55] Bergami AV, Forte A, Lavorato D, Nuti C. Proposal of a incremental modal pushover analysis (IMPA). Earthq Struct 2017;13(6):539–49.
[56] Fiorentino G, Forte A, Pagano E, Sabetta F, Baggio C, Lavorato D, et al. Central Italy earthquakes. Bull Earthq Eng 2016;2017:1–25.
[57] Resta M, Fiore A, Monaco P. Non-linear finite element analysis of masonry towers by adopting the damage plasticity constitutive model. Adv Struct Eng 2013;16(5):791–803.
[58] Fiore A, Monaco P. Earthquake-induced pounding between the main buildings of the “Quinto Orazio Flacco” school. Earthq Struct 2010;1(4):371–90.
[59] Fiore A, Spagnoletti G, Greco R. On the prediction of shear brittle collapse mechanisms due to the infill-frame interaction in RC buildings under pushover analysis. Eng Struct 2016;121:147–59.
[60] Colapietro D, Fiore A, Netti A, Fatiguso F, Marano GC, De Fino M, Cascella D, Ancona A. 2013. Dynamic identification and evaluation of the seismic safety of a masonry bell tower in the south of Italy. In: ECCOMAS Thematic Conference - COMPDYN 2013: 4th international conference on computational methods in structural dynamics and earthquake engineering, proceedings - an IACM special interest conference; 2013. p. 3459–70.
[61] Greco R, Marano GC. Site based stochastic seismic spectra. Soil Dyn Earthq Eng 2013;288–295.
[62] Vanmarcke EH, Gasparini DA. Compatible Simulated earthquake motions with prescribed answer will spectra. SIMQKE User' S manual and documentation. MIT R76-4 Carryforward; 1976.
[63] Rice SO. Mathematical analysis of random noise. Bell Syst Tech J 1994;23(3):282–332.
[64] Atkinson GM, Pierre JR. Ground-motion Response spectra in eastern North America for different critical damping values. Seismol Res Lett 2004;75(4):541–5.
[65] Stafford PJ, Mendis R, Bommer JJ. Dependence of damping correction factors for response spectra on duration and numbers of cycles. ASCE, J Struct Eng 2008;134:1364–73.
[66] MATLAB and Statistics Toolbox Release. The MathWorks, Inc., Natick, Massachusetts, United States; 2012b.
[67] Quaranta G, Fiore A, Marano GC. Optimum design of prestressed concrete beams using constrained differential evolution algorithm. Struct Multidiscip Optim 2014;49(3):441–53.
[68] Shih-Sheng PL. Statistical characterization of strong ground motions using power spectral density function. Bull Seismol Soc Am 1982;72(1):259–74.
[69] Mohraz B. The seismic design handbook- chapter 2 earthquake ground motion and response spectra. Springer Science & Business Media; 2012.